Available online at www.sciencedirect.com

SCIENCE DIRECT®

C. R. Physique 6 (2005) 23–32

COMPTES RENDUS PHYSIQUE

http://france.elsevier.com/direct/COMREN/

Self-organization on surfaces/Auto-organisation sur les surfaces

Formation of self-assembled quantum dots induced by the Stranski–Krastanow transition: a comparison of various semiconductor systems

Henri Mariette

CEA-CNRS group "Nanophysique et Semiconducteurs" : CNRS, laboratoire de spectrométrie physique, université J. Fourier-Grenoble I, and CEA, département de recherche fondamentale sur la matière condensée/SPMM, 17, avenue des Martyrs, 38054 Grenoble, France

Available online 12 January 2005

Presented by Guy Laval

Abstract

To account for the occurrence (or not) of the Stranski–Krastanow (SK) transition (two-dimensional to 3D change of surface morphology) during the epitaxial growth of various lattice-mismatched semiconductor systems, we present a simple equilibrium model taking into account not only the lattice mismatch, but also the dislocation formation energy and the surface energy. It demonstrates the importance of these parameters especially for II–VI systems such as CdTe/ZnTe and CdSe/ZnSe. For II–VIs indeed, as misfit dislocations are easier to form than in III–Vs (such as InAs/GaAs) or IV systems (Ge/Si), the 3D elastic transition is short-circuited by the plastic transition. Nevertheless, by lowering the surface energy cost, telluride and selenide quantum dots can also be grown as predicted by our model and as shown experimentally by reflection high-energy electron diffraction (RHEED), atomic force microscopy and optical measurements. This model is also applied to the case of GaN/AlN, before discussing its limits. ***To cite this article: H. Mariette, C. R. Physique 6 (2005).***
© 2004 Académie des sciences. Published by Elsevier SAS. All rights reserved.

Résumé

Formation de boîtes quantiques auto-assemblées lors de la transition Stranski–Krastanow : comparaison pour différents systèmes semiconducteurs. Pour rendre compte de l'apparition (ou non) d'une transition Stranski–Krastanow (variation de 2D à 3D de la morphologie de surface) lors de la croissance épitaxiée de divers semiconducteurs ayant des paramètres de maille différents, nous présentons un modèle à l'équilibre prenant en compte non seulement le désaccord de paramètre, mais aussi l'énergie de formation des dislocations et l'énergie de surface. Cette approche met en évidence l'importance de ces paramètres, en particulier dans le cas des semiconducteurs II–VI tels que CdTe/ZnTe et CdSe/ZnSe : en effet pour ces systèmes, puisque les dislocations sont plus faciles à former que dans le cas des semiconducteurs III–V (i.e. InAs/GaAs) ou IV–IV (i.e. Ge/Si), une transition plastique apparaît aux dépends de la transition élastique 3D. Cependant, en diminuant le coût en énergie de surface, des boîtes quantiques à base de tellures et séléniures peuvent être aussi obtenues. Ceci est mis en évidence expérimentalement par des mesures de diffraction en incidence rasante, de microscopie à force atomique, et de spectroscopie optique. Le modèle est ensuite appliqué au système GaN/AlN, et ses limites sont discutées. ***Pour citer cet article : H. Mariette, C. R. Physique 6 (2005).***
© 2004 Académie des sciences. Published by Elsevier SAS. All rights reserved.

E-mail address: mariette@drfmc.ceng.cea.fr (H. Mariette).

1631-0705/$ – see front matter © 2004 Académie des sciences. Published by Elsevier SAS. All rights reserved.
doi:10.1016/j.crhy.2004.11.003

Keywords: Quantum dots; Semiconductors; Molecular beam epitaxy

Mots-clés : Boîtes quantiques ; Semiconducteurs ; Épitaxie par jets moléculaires

1. Introduction

Some combinations of lattice-mismatched semiconductors can exhibit, under specific epitaxial growth conditions, a sharp transition from a layer-by-layer 2D growth to the formation of 3D islands. This Stranski–Krastanow (SK) growth mode [1] allows the relaxation of highly strained 2D layers through the stress-free facets of 3D islands instead of generating misfit dislocations (MDs) [2]. These islands are expected to be dislocation-free and are thus of high structural quality. Usually their typical sizes are on the scale of a few nanometers, so that these self-assembled quantum dots (QDs) are attractive nanostructures for the study of zero-dimensional effects. In particular the growth of these QDs, including the ability to tune their dimensions, their surface density and their positions, is nowadays a topic of intense research effort in order to control their optical properties for optoelectronic applications [3].

The formation, above a critical film thickness, of such QDs by molecular beam epitaxy (MBE) has been first discovered by Goldstein et al. [4] by observing in situ the 2D–3D morphology change of an InAs layer grown on GaAs; the process is now well established for this III–V semiconductor system [5]. The large lattice mismatch ($\Delta a/a \approx 7\%$) between these two semiconductors is seen as the driving force which induces the 2D–3D change of the surface morphology with the formation of SK islands. However, in the case of II–VI systems, which can exhibit mismatch as large as 6% for CdTe/ZnTe or CdSe/ZnSe, the 2D–3D transition is much less obvious: no clear 3D RHEED pattern has been reported during growth although zero-dimensional behavior was obtained [6–9]. In II–VIs indeed, above a critical thickness, MDs form easier than in III–Vs, as clearly observed for CdTe/ZnTe by Cibert et al. [10], which corresponds to a plastic relaxation as first considered by Frank and van der Merwe [2]. On the other hand, there are systems such as GaN/AlN [11] or SiGe/Si [12,13], with lower misfit (respectively 2.4% and less than 4%), which are known for exhibiting a clear SK transition with the formation of coherent islands.

There are therefore other parameters than the lattice mismatch in order to account for the 2D–3D transition. In this article a simple equilibrium model, taking into account not only the lattice mismatch but also the dislocation formation energy and the surface energy, is presented to explain the occurrence (or not) of this 2D–3D transition for various semiconductor systems. The limits of this approach are then discussed by giving some examples of the importance of kinetics effects.

2. Equilibrium model

This model allows us to reproduce the various types of growth modes observed in situ by RHEED during the MBE of heterostructures, namely: (i) a 2D-coherent growth mode; (ii) a SK-coherent mode with the formation of coherent SK islands only; (iii) a 2D-MD mode with only the formation of misfit dislocations; and (iv) a SK-MD mode with both SK islands and MD.

In the framework of linear elasticity, the film's free energy per unit area, $E = E_{\text{strained epilayer}} + E_{\text{surface}}$, can be written as a function of film's thickness h ($h > 1$ monolayer (ML)) for the four growth modes as follows:

$$E_{\text{2D-coh.}}(h) = M(\Delta a/a)^2 h + \gamma, \tag{1}$$

$$E_{\text{SK-coh.}}(h) = (1-\alpha)M(\Delta a/a)^2 h + \gamma + \Delta\gamma, \tag{2}$$

$$E_{\text{2D-MD}}(h,d) = (1-d_0/d)^2 M(\Delta a/a)^2 h + 2E_{\text{MD}}(h)/d + \gamma, \tag{3}$$

$$E_{\text{SK-MD}}(h,d) = (1-\alpha)(1-d_0/d)^2 M(\Delta a/a)^2 h + 2E_{\text{MD}}(h)/d + \gamma + \Delta\gamma, \tag{4}$$

where M is the film's biaxial modulus, $\Delta a/a$ the lattice mismatch between the epilayer and the substrate: $(a_{\text{subst.}} - a_{\text{epi.}})/a_{\text{epi.}}$, γ the film's surface energy ($<\gamma_{\text{subst.}}$), α the elastic gain in accommodating film's strain through the formation of partly relaxed SK islands, $\Delta\gamma$ the surface energy cost when creating facets ($\Delta\gamma = \gamma_{\text{SK}} - \gamma$), d the average distance between MDs at the film-substrate interface, d_0 that distance for a fully relaxed epilayer, d_0/d being the plastic gain in accommodating misfit with MDs, and E_{MD} the energy cost per unit length of forming a MDs. We consider that these MDs distribute themselves in a periodic two-dimensional crossed square array of non-interacting dislocations with a MDs length per unit film area of $2/d$. In the case of truncated regular pyramidal islands, $\Delta\gamma$ can be expressed very simply as a function of γ and γ_{F} (facets' surface energy) [14]: $\Delta\gamma = A(\gamma_{\text{F}}/\sin\theta - \gamma/\tan\theta)$, θ being the angle between the facets and the plane ((001) hereafter), and A a coefficient depending on both the QDs density and the QDs sizes (here A is normalized to one). Then, knowing dots' properties (θ, γ and γ_{F}), $\Delta\gamma$ can be calculated from the above equation and α estimated by atomistic calculation of the elastic relaxation

Table 1
Room temperature parameters [17] used in our calculations

	$\Delta a/a$ (%)	d_0 (Å)	M_{001} (GPa)	μ (GPa)	ν	$\Delta\gamma$ (meV/Å^2)	$E_{\text{c-MD}}$ (eV/Å)
InAs/GaAs	−6.7	32	79	34	0.3	5 (As-rich)	0.9
CdTe/ZnTe	−5.8	39	39	16	0.4	(Cd) 10 ∼ 4 (Te)	0.6
CdSe/ZnSe	−6.3	34	54	21	0.4	(Cd) 12 ∼ 4 (Se)	0.6

(see for example the valence force field model [15]). One should point out that $\Delta\gamma$ and α are related to each other, both depending on the shape of the QDs. In our approach, α was chosen constant, equal to 40% [16].

Let us note that Eqs. (3) and (4) are still dependent on both variables h and d. In the framework, however, of the MD equilibrium theory developed by Matthews [14], for a given film's thickness h, the free energy can be minimized for an optimal distance d between MDs obtained from: $\partial E_{\text{2D-MD}}$ or $_{\text{SK-MD}}/\partial d|_{h\ \text{constant}} = 0$.

By substituting these optimal values for d into Eqs. (3) and (4), they can be rewritten:

$$E_{\text{2D-MD}}(h) = -E_{\text{MD}}(h)^2/\big(M(\Delta a/a)^2 d_0^2 h\big) + 2E_{\text{MD}}(h)/d_0 + \gamma, \tag{5}$$

$$E_{\text{SK-MD}}(h) = -E_{\text{MD}}(h)^2/\big[(1-\alpha)M(\Delta a/a)^2 d_0^2 h\big] + 2E_{\text{MD}}(h)/d_0 + \gamma + \Delta\gamma. \tag{6}$$

These equations are only defined for a film thickness h above a critical value of $h_c^{\text{MD}} = E_{\text{c-MD}}/(M(\Delta a/a)^2 d_0)$ for Eq. (5) (where $E_{\text{c-MD}}$ is the MDs energy formation at the critical plastic thickness h_c^{MD}) and similarly for Eq. (6). Let us also note that from Eqs. (1) and (2), we can define an other critical thickness: $h_c^{\text{SK}} = \Delta\gamma/(M(\Delta a/a)^2\alpha)$ corresponding to the SK transition.

For a given epilayer thickness h, the equilibrium growth mode is the one exhibiting the minimum energy. The comparison between the energies deduced from Eqs. (1), (2), (5) and (6) will therefore enable us to predict which growth mode behavior is expected.

The different values used in the present calculations for the three zinc-blende systems studied hereafter, InAs/GaAs, CdTe/ZnTe and CdSe/ZnSe, all (001)-oriented, are listed in Table 1 [17]. We considered MD at the interface of kind 60°, that is with a Burgers vector b at 60° to the dislocation line and inclined at 45° to the (001)-interface. These are the most efficient complete MDs that can glide to the interface on the dense $\{111\}$ planes (either by bending a threading dislocation or by depositing a dislocation loop nucleated at the surface). Their Burgers vector is of type $\frac{1}{2}a\langle 110\rangle$, i.e. b is equal to $a/\sqrt{2}$ (where a is the lattice parameter of the strained film), but the misfit they accommodate is only half, $\frac{1}{2}b/d$, that accommodated by a pure edge MD with a Burgers vector lying in the interface [18]. Considering 60° MD, d_0 is therefore equal to $a/(2\sqrt{2}|\Delta a/a|)$.

The energy cost E_{MD} required for creating a unit length 60°-MD at the interface is given by $[\ln(h/b)+1] \times \mu b^2(1-\nu/4)/[4\pi(1-\nu)]$ [19], where μ is the shear modulus at the interface between the film and the substrate (μ is equal to $(C_{11} - C_{12} + C_{44})/3$ for the slip system $\langle 011\rangle\{111\}$) and ν Poisson's ratio. Using the above formula, E_{MD} has been calculated as a function of h [20]: the main result is that MDs are really easier to form in II–VIs than in III–Vs, which is a major clue for understanding why, at misfit as large as 6%, systems such as InAs/GaAs exhibit a SK transition whereas others, such as CdTe/ZnTe or CdSe/ZnSe, rather do not.

3. Results

Fig. 1 reports the film's free energy for the four different growth modes in the case of InAs/GaAs (001) as a function of layer thickness h. As the growth proceeds, h increases, the initial 2D-coherent growth mode changes into the SK one when the layer thickness h exceeds a critical value $h_{\text{crit.}}^{\text{SK-coh.}}$ of 1.7 MLs (elastic relaxation). This result is in good agreement with the experimental ones reported in the literature (see for example Gérard et al. [21]). Then, above a second critical thickness, $h_c^{\text{SK-MD}}$ of about 8 ML, islands' growth (either when reaching a critical volume or when coalescing) leads to the formation of MDs: SK-MD growth mode. Finally, above 20 MLs, the 2D-MD growth mode predominates.

Fig. 2 shows the film's free energies for the various growth modes in the case of both CdTe/ZnTe (Fig. 2 (a) and (b)) and CdSe/ZnSe (Fig. 2 (c) and (d)). As the growth proceeds, the initial 2D-coherent growth mode changes into the 2D-MD mode when the layer thickness h exceeds a critical value h_c^{MD} of about 5 monolayers (MLs). This is confirmed by the observation in situ of a streaky RHEED pattern as previously reported for CdTe/ZnTe (see for example Cibert et al. [10]). Note that this behavior contrasts with that predicted [20] and observed [21] for InAs/GaAs (001): in this case the transition which occurs first is the elastic one, with the formation of coherent islands at a critical thickness h_c^{SK} of about 1.7 ML.

The different behavior between the two types of systems, II–VIs as compared to III–Vs, is mainly due to the lower values of E_{MD} for the former. Indeed, by considering the ratio η between the two critical thicknesses, h_c^{MD} and h_c^{SK}, one can write

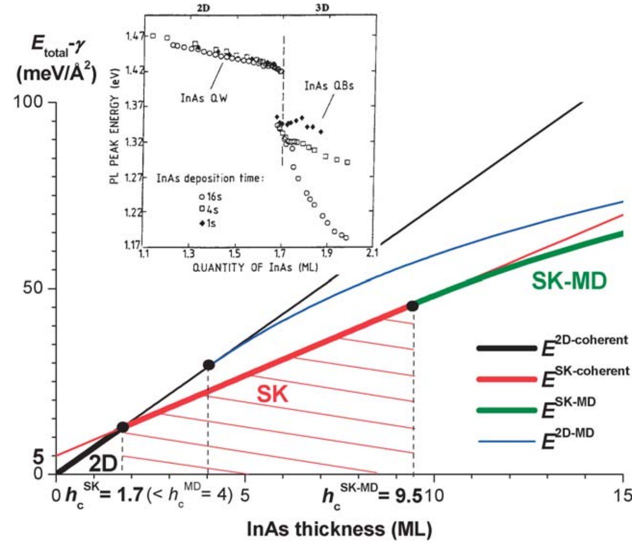

Fig. 1. InAs/GaAs film's free energy per unit area for the four possible growth modes as a function of InAs thickness. The bold lines correspond to the equilibrium growth modes, namely: 2D until 1.7 ML (in agreement with experimental data of Gérard et al. [21], see the insert), then SK until 7.8 ML (hatched area), and finally SK-MD.

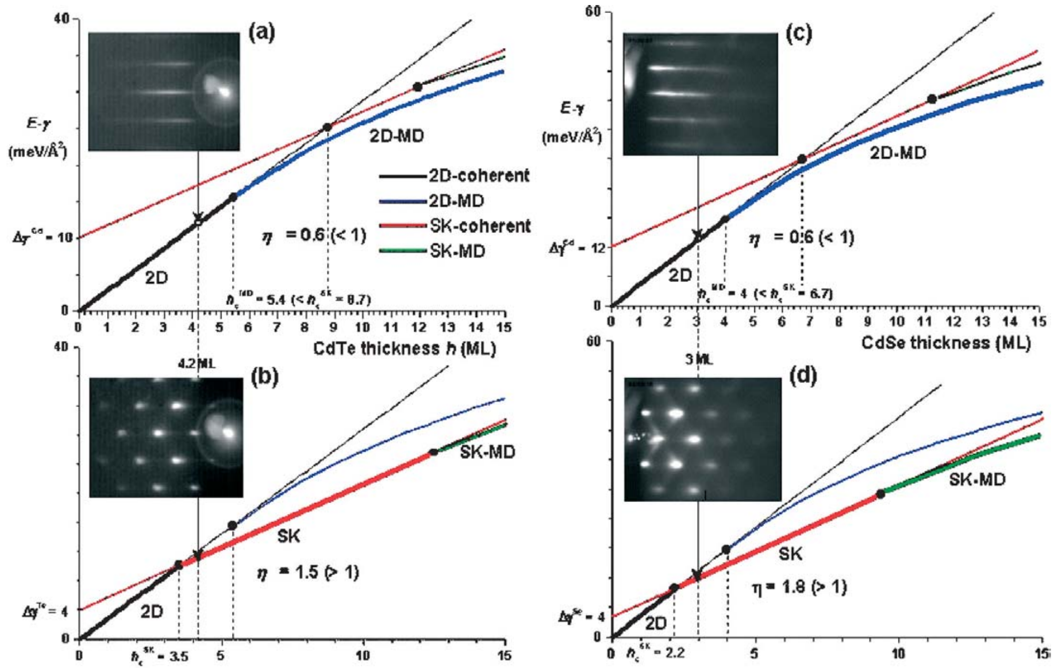

Fig. 2. CdTe/ZnTe (respectively CdSe/ZnSe) – (001) film's free energy as a function of CdTe (CdSe) thickness h. The experimental RHEED pattern in the inserts correspond, for (a) and (c), to Cd (Se)-rich growth conditions, and for (b) and (d), to a post growth treatment, namely the deposition and desorption of a thin amorphous Te (Se) layer. The spotty RHEED after such a treatment is a direct fingerprint of the SK transition. It can be understood as a decrease of the surface energy cost $\Delta\gamma$ as illustrated with the equilibrium model applied for both CdTe/ZnTe and CdSe/ZnSe systems. The bold lines correspond to the growth modes expected with our model assuming a decrease of the surface energy cost $\Delta\gamma$ by a factor 3 (respectively 4) when going from cation-rich surfaces to anion-rich ones.

$\eta = h_c^{MD}/h_c^{SK} \propto E_{c\text{-MD}}|\Delta a/a|/\Delta\gamma$ which predicts which growth mode will occur first (see Fig. 4). For the II–VI systems, the low value of E_{MD} favors plastic relaxation ($\eta < 1$). However, by decreasing the surface energy cost $\Delta\gamma$ for creating facets, it should be possible to fulfill the condition $\eta > 1$ and to induce the SK transition before the plastic one.

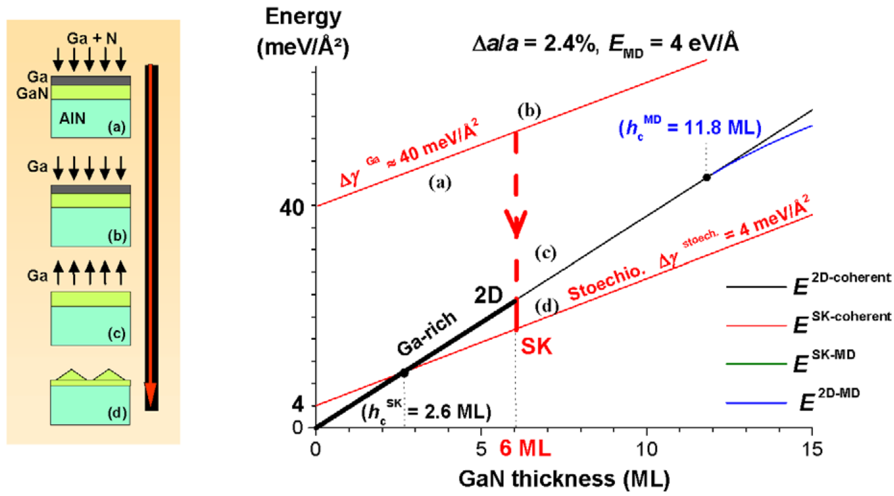

Fig. 3. GaN/AlN-(0001) film's free energy as a function of GaN thickness h. Scheme of the four steps (a) to (d) done experimentally to induce the SK transition are presented on left-hand side [31] and illustrated on the growth diagram.

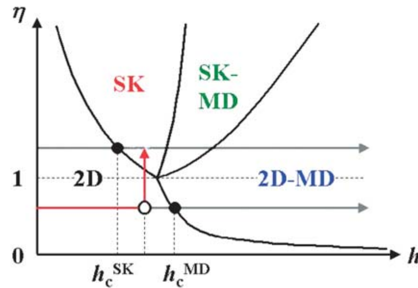

Fig. 4. Schematic diagram illustrating the growth modes as a function of the deposited material and the ratio of critical thicknesses. The grey horizontal line corresponds to InAs/GaAs, the red one to the II–VI's and GaN/AlN grown with an excess of Ga. $\eta = (h_c^{MD}/h_c^{SK}) \propto (E_{c\text{-}MD}|\Delta a/a|/\Delta\gamma)$.

Such a decrease of the surface energy has been experimentally obtained through various growth procedures: (i) by depositing amorphous tellurium (respectively selenium) onto a 4.2 ML CdTe layer [22] (respectively CdSe [23]), that is just below its plastic relaxation thickness. The 2D–3D transition is then observed after desorbing this amorphous tellurium (selenium) at 220 °C (i.e. below CdTe (CdSe) growth temperature at 300 °C), as revealed by a clear 3D RHEED pattern (see inset of Fig. 2(b)). (ii) By using II–VIs' atomic layer epitaxy (ALE) [24,25]: ALE indeed allows us to establish, after each flux sequence (successively Cd and then Te or Se), an equilibrium corresponding to a given surface reconstruction which minimizes the surface energy and so favors the SK transition as observed for CdTe by RHEED [26]. (iii) By annealing for twenty minutes at 340 °C under Se flux a CdSe layer, which also leads to a 3D RHEED pattern [27]. If we consider that these processes decrease the surface energy variation $\Delta\gamma$ by a factor 2, we can account for the observed experiments (Fig. 2 (b) and (d)).

The expected decrease of $\Delta\gamma$ on exposing the II–VI layer to a large quantity of the group-VI element corresponds to an increase, to first order, of the 2D surface energy γ, whereas γ_{SK} is not expected to vary as much as γ due to the similar shape and aspect ratio of all self-assembled QDs. This can be understood qualitatively as follows: Under an excess of Te (Se), the surface reconstruction of CdTe (CdSe) corresponds to a coverage of Te (Se) equal to 1, in contrast to the coverage of a Cd-rich surface, equal to 0.5 [28]. So a Te (Se)-rich II–VI surface can be considered to be more ionic and is expected to have a larger surface energy γ. Thus, the energy cost $\Delta\gamma$ for creating facets is lowered, favoring the SK transition. This interpretation needs confirmation by ab initio calculations of the variations of the surface energy.

For another small lattice mismatch system, namely GaN/AlN ($\Delta a/a = -2.4\%$) surface energies were calculated ab initio [29] in the presence (or not) of a Ga-bilayer on the growth front. Such data allow us to account for the results obtained experimentally: in the presence of an excess of Ga, the GaN layer stays 2D [30] whereas, by stopping the growth and evaporating this excess of Ga, a clear SK transition occurs [31]. This corresponds to a decrease of the surface energy cost from $\Delta\gamma^{Ga}$ to $\Delta\gamma^{N}$ as calculated by Neugebauer et al. [29] which induces the SK transition (Fig. 3).

In such results, the Ga can be seen as an self-surfactant, an effect which was already well documented for InAs/GaAs [32]. However, by contrast with the interpretation usually proposed which is a kinetic effect (the presence of the surfactant limits the mobility of the adatoms onto the surface and then inhibits the formation of islands), we show here the thermodynamical action of the surfactant, that is the increase of the surface energy cost for creating facets.

It is interesting to note that the SK transition of GaN on AlN could be induced directly during the growth by working in the N-rich conditions [30].

In summary, we have induced for the II–VI and nitrides QDs a 2D–3D transition, which occurs *after and not during growth* by the rearrangement of a strained 2D layer. This morphology transition under a fixed amount of deposited material (Fig. 4) can be understood as a surface energy variation obtained by exposing the II–VI layer to a large quantity of the group-VI element, or by evaporating the excess of Ga present at the growth front of a GaN epilayer. This method allows us in principle to grow QDs with less amount of material than that predicted by the critical thickness for a SK transition occurring during the growth (Fig. 4). Moreover, it opens the way toward the growth of QDs with two materials having even a smaller mismatch $\Delta a/a$, provided that it is possible to decrease sufficiently the surface energy cost $\Delta\gamma$.

In the next section we will discuss some experimental results showing the characteristics of the QDs obtained with this method (red path on Fig. 4) by comparison with the standard one (grey path). Moreover, we will give some examples that show the influence of the kinetics effects in the formation of these QDs, effects which are not taken into account in the previous approach.

4. Discussion

Fig. 5 shows the evolution of the QDs density for the three cases presented above: (i) the InAs/GaAs system with a standard SK transition induced during the growth by changing the InAs coverage; (ii) the CdTe/ZnTe system by changing the surface energy for three different CdTe coverages; (iii) the GaN/AlN system with the two methods, either by changing the surface energy (open squares) or directly during the growth (full circles). The standard SK transition gives rise to a very strong variation of the QDs density when changing only by a fraction of monolayer the material coverage [33]. Such density variation has been modelled as a function of InAs coverage with a power law having an exponent m of the order of 1.8 [5]. The result emphasizes the difficulty of controlling precisely the QDs density knowing that a small imprecision of the amount of InAs deposited is always present in a MBE system. As far as the QDs shape is concerned, a transition has been observed by scanning tunneling microscopy between two types of InAs islands having two distinct faceted shapes [34]: such transition can be understood as a natural consequence of the strain and surface energies scaling differently as a function of island volume. Several models have been developed in order to explain such shape transitions in epitaxially strained islands [35–38] based for example on the various minimum energy configurations represented by the different islands shapes as a function of the volume [38].

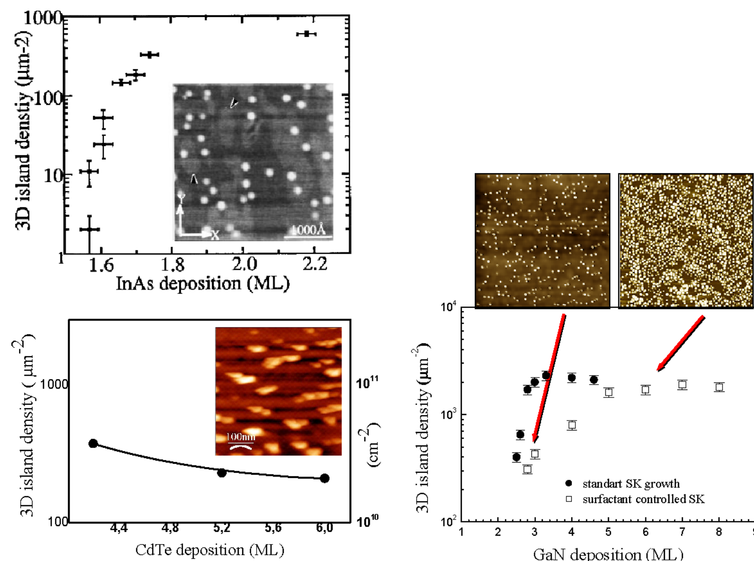

Fig. 5. 3D islands densities versus deposited material (in monolayers) and AFM images for three systems: InAsGaAs with a standard SK growth [32], CdTe/ZnTe by changing the surface energy [20], and GaN/AlN with both processes [30].

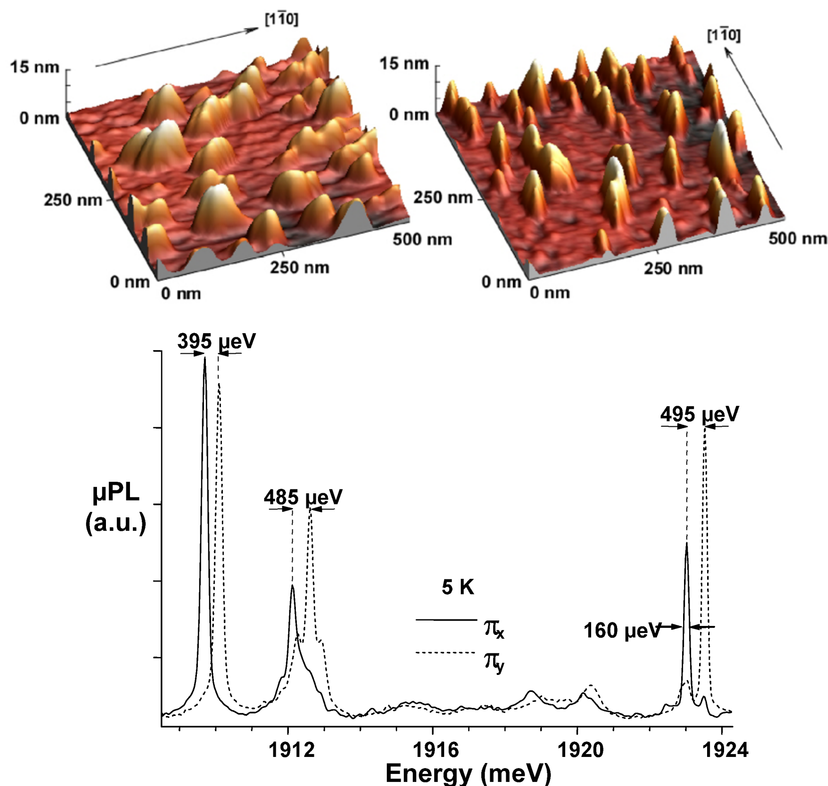

Fig. 6. UHV-AFM images of CdTe QDs showing for the two scan directions a preferential orientation along the [1 −1 0] axis. Linearly polarized μPL along the ⟨110⟩ crystallographic axes of single CdTe QDs encapsulated in $Zn_{0.8}Mg_{0.2}Te$ [22].

By contrast, when the SK transition is induced by a surface energy change, the density variation is less abrupt (see the results for GaN on Fig. 5) or even smooth in the case of CdTe (Fig. 5). As far as the nitrides are concerned, the QDs density can be controlled over about one order of magnitude (from 3×10^{10} cm^{-2} to 2×10^{11} cm^{-2}) for coverages ranging from 2.8 to 6 MLs [31]. For comparison, the density of GaN QDs grown in the standard SK mode saturates at 2×10^{11} cm^{-2} for a coverage of only 3 MLs. For both methods, the QDs shape is similar, namely a hexagonal truncated pyramid with [1–130] facets inclined by 32° with respect to the (0001) plane. However, for the surfactant controlled SK growth mode, the aspect ratio (height/diameter) increases from $1/8$ to $1/5$ for GaN coverage varying from 2.8 to 8 MLs [31].

For CdTe, the QDs density variation when changing the coverage by 50% is even smaller (Fig. 5). The increase of CdTe amount leads to an increase of the dots size as observed by UHV-AFM images and no clear shape transition is observed. However there is a tendency to have anisotropic islands. Fig. 6 shows some characteristics of these CdTe uncapped QDs. The dots present a clear anisotropy with an elliptic shape. They are preferentially oriented along the [1 −1 0] axis as illustrated in the figure. This anisotropy accounts for the splitting of individual emission lines of capped QDs studied by linearly polarized micro-photoluminescence (μPL) [22,25] as also reported for InAs [39]and CdSe QDs [40]. Their average base major (minor) axis is 50 nm (respectively 30 nm) and their average aspect ratio varies from 1/8 to 1/10, values similar to those reported for III–V semiconductor systems.

To summarize, these variations of both QDs density and shape show that more sophisticated models have to be developed in order to account for the experimental data. The variation of the shape as a function of the material coverage clearly demonstrated the importance of the relative values of γ_F which could lead to various configurations as a function of the QDs volume. The variation of the QDs density points out also the strong influence of the kinetic effects: depending on the mobility of the adatoms, the formation of the QDs can be either inhibited or increased.

These kinetic effects are illustrated in Fig. 7. The growth mode of GaN onto AlN buffer depends on the substrate temperature [11] (Fig. 7): at low temperature (below 690 °C) there is a 2D growth mode with a dynamic formation of 2D platelets [41] and a gradual relaxation of the layer by introducing misfit dislocations when the GaN thickness increases. Instead, at higher temperature (above 700 °C), the SK growth mode prevails as observed on Fig. 7. Such behavior has been explained in terms of Ga surface diffusion variation: the substrate temperature can activate the adatoms' mobility in order to allow the formation

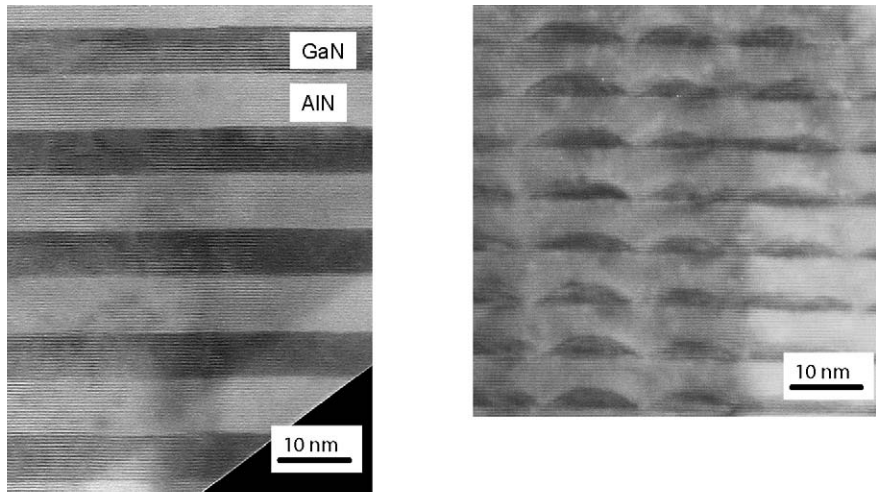

Fig. 7. High resolution transmission electron microscopy of GaN/AlN heterostructures grown by N_2 plasma assisted MBE either at 620 °C (2D superlattice on the left-hand side), or at 710 °C (GaN quantum dots on the right-hand side) [11].

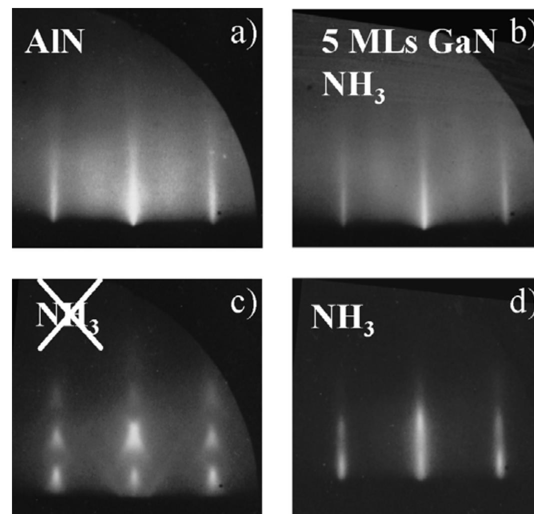

Fig. 8. RHEED patterns obtained during the MBE growth of GaN on AlN at 800 °C using NH_3 as nitrogen source [42]. The 2D RHEED of 5MLs GaN under NH_3 can be explained with the calculated values of H-rich surfaces energies ($\Delta\gamma = 17\ \text{meV}/\text{Å}^2$), whereas the 3D one under vacuum (c) corresponds to stoechiometry surfaces values ($\Delta\gamma = 4\ \text{meV}/\text{Å}^2$). The reversibility of the 2D–3D transition is demonstrated by the re-apparition of a 2D RHEED when re-exposing to NH_3.

of the dots [11, 41 and references therein]. The importance of such kinetics effects are not taken into account in the simple approach presented above which assumes that the growth occurs close to the thermodynamical equilibrium.

However, to justify this assumption, Fig. 8 shows a result which clearly demonstrates in situ the reversibility of the 2D–3D transition [42]. In this case the MBE growth of GaN on AlN is done using NH_3 as nitrogen source: for NH_3 rich conditions: a 2D growth mode occurs with an excess of ammonia, whereas, by shuttering the NH_3 flux, a 2D–3D transition is induced. Moreover if the sample is exposed again to the NH_3 flux, the surface morphology turns into a 2D one again as revealed in situ by the RHEED pattern. Using the surface energy values mentioned in Fig. 8, we can account for the growth mode change under these conditions.

Let us point out also the experimental results of Fig. 1 which demonstrate that the onset of the SK transition, for given conditions, is not driven by the growth rate: indeed the emission of the dots, (and then their size) strongly depends on the time to deposit a given InAs amount, but the onset of 2D–3D transition always occurs for the same critical thickness, namely 1.7 ML of InAs.

5. Summary

We have developed an equilibrium model allowing us to account for the epitaxial growth modes of various lattice-mismatched semiconductor systems. This model considers the formation of SK islands and/or misfit dislocations. It demonstrates the importance of various parameters in determining the growth morphology, namely the lattice mismatch, the dislocation formation energy and the surface energy. In particular for II–VI semiconductors the dislocation formation energy being lower than in the III–Vs, the plastic relaxation (2D-MD) is more favorable than the elastic one (SK). However, by decreasing the surface energy, which was done under an excess of metalloids (Te or Se), one can induce the SK growth mode, as experimentally confirmed by RHEED, and thus form II–VI QDs. This model, however, describes the growth behavior at the equilibrium. In fact kinetics effects (mobility of adatoms, of dislocations) can also play an important role during the hetero-epitaxy of such mismatched systems. This influences also the QDs shape, their density, and even their formation. For example, the substrate temperature can activate or not adatoms' mobility in order to form (or not) the QDs. Finally the challenge nowadays is to control precisely both the position and electronic properties of the dot onto the surface (see for example [43,44]) which is a pre-requirement to ultimately use these dots in quantum devices.

Acknowledgements

We would like to thank our colleagues from the CEA-CNRS group "Nanophysique et Semiconducteurs", C. Adelmann, R. André, J. Cibert, B. Daudin, Y. Genuist, J.M. Gérard, N. Gogneau, K. Kheng, Le Si Dang, S. Moehl, E. Monroy, I.C. Robin, S. Tatarenko, M. Terrier, and last but not least F. Tinjod with whom this model was developed. We acknowledge also J. Neugebauer (Paderborn University) for the collaboration about surface energy calculations.

References

[1] I.N. Stranski, L. Krastanow, Ber. Akad. Wiss. Wien, Math.-Naturwiss. Kl., Abt. IIb 146 (1938) 797.
[2] F.C. Frank, J.H. van der Merwe, Proc. Roy. Soc. London Ser. A 198 (1949) 216.
[3] See for example J.M. Gérard, in this issue.
[4] L. Goldstein, F. Glas, J.Y. Marzin, M.N. Charasse, G. Le Roux, Appl. Phys. Lett. 47 (1985) 1099.
[5] See for example J.-Y. Marzin, J.-M. Gérard, A. Izrael, D. Barrier, G. Bastard, Phys. Rev. Lett. 73 (1994) 716;
D. Leonard, K. Pond, P.M. Petroff, Appl. Phys. Lett. 50 (1994) 11687;
R. Nötzel, Semicond. Sci. Technol. 11 (1996) 1365.
[6] Y. Terai, S. Kuroda, K. Takita, T. Okuno, Y. Masumoto, Appl. Phys. Lett. 73 (1998) 3757.
[7] G. Karczewski, S. Mackowski, M. Kutrowski, T. Wojtowicz, J. Kossut, Appl. Phys. Lett. 74 (1999) 3011.
[8] S.H. Xin, P.D. Wang, A. Yin, C. Kim, M. Dobrowolska, J.L. Merz, J.K. Furdyna, Appl. Phys. Lett. 69 (1996) 3884.
[9] D. Schikora, S. Schwedhelm, D.J. As, K. Lischka, D. Litvinov, A. Rosenauer, D. Gerthsen, M. Strassburg, A. Hoffmann, D. Bimberg, Appl. Phys. Lett. 76 (2000) 418.
[10] J. Cibert, Y. Gobil, Le Si Dang, S. Tatarenko, G. Feuillet, P.H. Jouneau, K. Saminadayar, Appl. Phys. Lett. 56 (1990) 292.
[11] F. Widmann, J. Simon, B. Daudin, G. Feuillet, J.L. Rouvière, N.T. Pelekanos, G. Fishman, Phys. Rev. B 58 (1998) 15989;
C. Adelmann, M. Arlery, B. Daudin, G. Feuillet, G. Fishman, Le Si Dang, H. Mariette, N.T. Pelekanos, J.L. Rouvière, J. Simon, F. Widmann, C. R. Acad. Sci. Paris, Ser. IV 1 (2000) 61.
[12] Vinh Le Thanh, V. Yam, P. Boucaud, F. Fortuna, C. Ulysse, D. Bouchier, L. Vervoort, J.-M. Lourtioz, Phys. Rev. B 60 (1999) 5851.
[13] G. Capellini, L. Di Gaspare, F. Evangelisti, E. Palange, Appl. Phys. Lett. 70 (1997) 493.
[14] J. Tersoff, R.M. Tromp, Phys. Rev. Lett. 70 (1993) 2782.
[15] C. Priester, M. Lannoo, Phys. Rev. Lett. 75 (1995) 93, and references therein.
[16] D. Bimberg, M. Grundmann, N.N. Ledensov, Quantum Dot Heterostructures, Wiley, 1999, p. 43.
[17] Landolt-Börnstein, Springer-Verlag, Berlin, 1982, vol. III/17a and b, and references therein.
[18] J.W. Matthews, J. Vac. Sci. Technol. 12 (1975) 126.
[19] E.A. Fitzgerald, Mater. Sci. Rep. 7 (1991) 87.
[20] F. Tinjod, PhD Thesis, Univ. J. Fourier, Grenoble, France, 2003;
F. Tinjod, I. Robin, R. André, K. Kheng, H. Mariette, in: Fall Meeting Eur. Mat. Soc., Zakopane, Poland, October 2002, J. Alloys Compd. 371 (2004) 63.
[21] J.-M. Gérard, J.B. Génin, J. Lefebvre, J.M. Moisson, N. Lebouché, F. Barthe, J. Cryst. Growth 150 (1995) 351.
[22] F. Tinjod, B. Gilles, S. Moehl, K. Kheng, H. Mariette, Appl. Phys. Lett. 82 (2003) 4340.
[23] I.C.. Robin, R. André, H. Mariette, S. Tatarenko, Le Si Dang, J.M. Gérard, in: 3rd Int. Conf. Quantum Dots, Banff, 2003, Phys. E, in press.
[24] J.-M. Hartmann, G. Feuillet, M. Charleux, H. Mariette, J. Appl. Phys. 79 (1996) 3035.
[25] L. Marsal, L. Besombes, F. Tinjod, K. Kheng, A. Wasiela, B. Gilles, J.-L. Rouvière, H. Mariette, J. Appl. Phys. 91 (2002) 4936.
[26] H. Mariette, L. Marsal, L. Besombes, F. Tinjod, B. Gilles, K. Kheng, J.-L. Rouvière, J. Cryst. Growth 237/239 (2002) 227.

[27] M. Rabe, M. Lowisch, F. Henneberger, J. Cryst. Growth 184/185 (1998) 248.
[28] M.B. Veron, M. Sauvage-Simkin, V. Etgens, S. Tatarenko, H. van der Vegt, S. Ferrer, Appl. Phys. Lett. 67 (1995) 3957.
[29] C.G. Van de Walle, J. Neugebauer, Phys. Rev. Lett. 88 (2002) 066103;
J. Neugebauer, Private communication.
[30] C. Adelmann, J. Brault, D. Jalabert, P. Gentil, H. Mariette, G. Mula, B. Daudin, J. Appl. Phys. 91 (2002) 9638.
[31] C. Adelmann, N. Gogneau, E. Sarigiannidou, J.-L. Rouviere, B. Daudin, Appl. Phys. Lett. 81 (2002) 3064;
N. Gogneau, D. Jalabert, E. Monroy, T. Shibata, M. Tanaka, B. Daudin, J. Appl. Phys. 94 (2003) 2254.
[32] See for example N. Grandjean, J. Massies, V.H. Etgens, Phys. Rev. Lett. 69 (1992) 796;
E. Tournié, K.H. Ploog, Thin Sol. Films 231 (1993) 43.
[33] N.P. Kobayashi, T.R. Ramachandran, P. Chen, A. Madhukar, Appl. Phys. Lett. 68 (1996) 3299.
[34] J.B. Smathers, C.L. Workman, H. Yang, P. Ballet, G.J. Salamo, Private communication.
[35] J. Tersoff, R.M. Tromp, Phys. Rev. Lett. 70 (1993) 2782.
[36] I. Daruka, J. Tersoff, A.L. Barabasi, Phys. Rev. Lett. 82 (1999) 2753.
[37] F.M. Ross, J. Tersoff, R.M. Tromp, Phys. Rev. Lett. 80 (1998) 984.
[38] G. Medeiros-Ribeiro, A.M. Bratkovski, T.I. Kamins, D.A. Ohlberg, R.S. Williams, Science 279 (1998) 353.
[39] M. Bayer, A. Kuther, A. Forchel, A. Gorbunov, V.B. Timofeev, F. Schäfer, J.P. Reithmaier, S.N. Walck, Phys. Rev. Lett. 82 (1999) 1748.
[40] V.D. Kulakovskii, G. Bacher, R. Weigand, T. Kümmell, A. Forchel, E. Borovitskaya, K. Leonardi, D. Hommel, Phys. Rev. Lett. 85 (1999) 1780.
[41] A. Bourret, C. Adelmann, B. Daudin, G. Feuillet, G. Mula, Phys. Rev. B 63 (2001) 245307.
[42] B. Damilano, PhD thesis, Univ. Nice-Sophia Antipolis, 2001;
B. Damilano, N. Grandjean, F. Semond, J. Massies, M. Leroux, Appl. Phys. Lett. 75 (1999) 962.
[43] S. Watanabe, E. Pelucchi, B. Dwir, M.H. Baier, K. Leifer, E. Kapon, Appl. Phys. Lett. 84 (2004) 2907.
[44] J. Eymery, G. Biasiol, T. Ogino, in this issue.